

# TAT-Beclin1 Represses the Carcinogenesis of DUSP4-positive PTC by Enhancing Autophagy

Leilei Zang

Second Hospital of Hebei Medical University

Yanmei Song

Hebei People's Hospital

Yanhua Tian

Second Hospital of Hebei Medical University

Ning Hu (✉ [HNhbm2@126.com](mailto:HNhbm2@126.com))

Second Hospital of Hebei Medical University <https://orcid.org/0000-0003-0258-9712>

---

## Research

**Keywords:** PTC, DUSP4, TAT-Beclin1, Autophagy, Beclin1

**Posted Date:** April 8th, 2021

**DOI:** <https://doi.org/10.21203/rs.3.rs-393413/v1>

**License:**   This work is licensed under a Creative Commons Attribution 4.0 International License.

[Read Full License](#)

---

# Abstract

**Background:** DUSP4 is a pro-tumorigenic molecule of papillary thyroid carcinoma (PTC). DUSP4 also exists as an autophagic regulator. Moreover, DUSP4, as a negative regulator of MAPK, can prevent Beclin1 from participating in autophagic response. This study aimed to explore whether TAT-Beclin1, a recombinant protein of Beclin1, could inhibit the tumorigenesis of DUSP4-positive PTC by regulating autophagy.

**Methods:** First, we divided PTC cancer tissues into three groups according to DUSP4 expression levels by immunohistochemical analyses, and evaluated the relationship between the expression of autophagic proteins (Beclin1 and LC3II) and DUSP4 expression using Western blotting assays. After overexpression of DUSP4 by lentiviral transduction, the roles of TAT-Beclin1 on DUSP4-overexpressed PTC was detected.

**Results:** Our results showed that the expression levels of autophagic proteins (Beclin1 and LC3II) increased with the increase of DUSP4 expression in PTC carcinomas. In PTC cells, DUSP4 overexpression-inhibited autophagic activity (including Beclin1 expression, LC3 conversion rate and LC3-puncta formation) and -promoted cell proliferation and migration were reversed by TAT-Beclin1 administration. *In vivo* assays also showed that DUSP4-overexpressed PTC cells had stronger tumorigenic ability and weaker autophagic activity, which was recovered by TAT-Beclin1 administration.

**Conclusions:** TAT-Beclin1, as an autophagic promoter, could repress the carcinogenesis of DUSP4-positive PTC, which implies that the addition of TAT-Beclin1 may be determined through detecting the levels of DUSP4 in the treatment of PTC.

## Introduction

The incidence rate of papillary thyroid carcinoma is 70%~80% in thyroid carcinoma [1]. The tumours of PTC patients grow slowly, show multifocal, and have a tendency of local lymph node metastasis. Nevertheless, some PTCs are highly aggressive and easy to dedifferentiate, which eventually develops into poorly differentiated or undifferentiated carcinoma. These above results have quite a negative impact on the survival rate and quality of life of PTC patients. There are lots of biomarkers, which have significant value on predicting the prognosis and therapeutic effect in PTC patients. However, the significance of a large proportion of biomarkers keeps vague in PTCs. Accordingly, it is of great significance to deepen the research on biomarkers related to PTC, on the basis of which the diagnosis and treatment of PTC could be further improved.

Dual specificity phosphatase 4 (DUSP4), a member of the bispecific phosphatase family, negatively regulates the activity of mitogen-activated protein kinase (MAPK) [2]. DUSP4 is considered a biomarker of lots of malignant tumours. The alteration of DUSP4 expression is related to the carcinogenesis of multiple tumours. DUSP4 is considered as the anti-oncogenic gene of most tumours [2–4], whilst serves as the pro-oncogenic gene of a small number of tumours, including PTC [5–7]. DUSP4 expression levels in PTC tissues is significantly higher than that in Paracancerous normal tissues [7]. The high expression

of DUSP4 is not only associated with lymph node metastasis and extrathyroid infiltration, but also an independent risk factor for lymph node metastasis [7]. Therefore, DUSP4 is considered a significant biomarker of PTC. However, the effect of DUSP4 on the diagnosis and treatment of PTC is still unclear.

Autophagy is a highly conserved cellular homeostasis mechanism. Moderate autophagy serves as a protective mechanism, i.e., protective autophagy, whilst excessive autophagy promotes cell death, i.e., autophagic cell death [8]. The inhibition of autophagic response on tumor cell survival has been reported in several studies [9–11]. Previous study showed that overexpression of DUSP4 in primary tissue and cell culture models of myocardium leads to the impairment of autophagy [12]. The similar result was also reported in the study of hepatocytes [13]. DUSP4 is a negative regulator of MAPK and can inhibit the activities of c-Jun N-terminal kinase (JNK), p38 and extracellular regulated protein kinase (ERK) [2, 14–16]. JNK is an important autophagy promoter under various stress and pathological conditions [17–20]. JNK can also promote cell death by activating autophagy, which is reflected in some malignant tumours [21–23]. Activated JNK is known to dissociate the autophagy molecule Beclin1 from BCL2-Beclin1 complex, and free Beclin1 can activate autophagy after entering autophagy flux [17]. Previous studies have also confirmed that JNK represses tumor growth by Beclin1-dependent autophagy activation [24, 25]. Remarkably, DUSP4 signal can inactivate MAPKs including JNK, which results in the decrease of Beclin1 expression and autophagic activity [13]. The latest research also confirms that DUSP4 exerts an inhibitory effect on JNK-Beclin1-autophagy activation signaling pathway [26]. Overall, we hypothesized that DUSP4-positive PTC may be sensitive to the treatment of Beclin1 recombinant protein, TAT-Beclin1.

The present study demonstrated that DUSP4-inhibited autophagic responses and –promoted proliferation, migration, tumorigenicity *in vivo* of PTC cells were all reversed by treatment of TAT-Beclin1. Therefore, through the combination of autophagy and potential biomarker in PTC, this study provided the first evidence for the application of Beclin1 recombinant protein in the treatment of PTC.

## Methods

### Clinical tissue specimens

A total of 45 pairs of PTC cancer tissues were obtained with written informed consent via surgical resection at The Second Affiliated Hospital of Hebei Medical University, Shijiazhuang, Hebei, China from May 2016 to February 2020. All tissue specimens were histopathologically examined by three independent pathologists. Fresh tissue specimens were frozen in liquid nitrogen and stored at -80 °C until utilization. All the clinical samples were acquired with informed consent from the participants. The Institutional Review Board of The second hospital of Hebei Medical University reviewed and approved this study (2016-R269). The clinical studies were conducted according to the principles expressed in the Helsinki Declaration.

### Cell lines and culture

The PTC cell lines TPC-1 and K1 were from American Type Culture Collection (ATCC). Cells were incubated in RPMI-1640 Medium (Thermo Fisher Scientific; Waltham, MA, USA) supplemented with 10% fetal bovine serum (FBS, Thermo Fisher Scientific). All cells were kept in humidified air at 37 °C and 5% CO<sub>2</sub>.

### **Experimental protocol of TAT-Beclin1 peptide**

TAT-Beclin1 peptide is a known autophagy inducer [27-29]. The cell permeable TAT-Beclin1 peptide was obtained from the Peptide Core at the University of Colorado Anschutz Medical Campus. The sequence of the TAT-Beclin1 peptide was RRRQRRKRGYGGDHWIHFTANWV [27]. In *in vitro* experiments, cells were treated with TAT-Beclin1 or vehicle (normal saline) at a dose of 10 µM. Tumor-bearing mice were treated with TAT-Beclin1 or vehicle via intraperitoneal injection (I.P.) at a dose of 20mg/kg/day.

### **Lentiviral Transduction**

Recombinant lentiviruses encoding DUSP4 were constructed by homologous recombination between the expression vector (pEX-Puro-Lv105) and cDNA in 293 cells as previously described using the lentivirus construction kit (GeneCopoeia) [30]. The same method was used to construct and package the corresponding control vector. After 2 days, supernatants were collected, and cells were incubated in medium containing lentiviruses at a multiplicity of infection (MOI) of 25 for 2 d. The infected cells were selected using puromycin (5 µg/ml). The overexpression efficiency of viral gene was detected using qPCR analysis.

### **siRNA Transfection**

Control siRNAs or siRNAs against human DUSP4 were obtained from Thermo Fisher Scientific. The target sequences were as following:

Control, 5'-CCCATCCTTCAACGAGCAT-3',

DUSP4, 5'-CCCAGTACCTTACCAGCAT-3'.

The indicated cells were cultured in 6-well plates and then transfected with siRNAs (100 pmol/well) using RNAiMAX (Thermo Fisher Scientific) in accordance with manufacturer's protocols. For 48 hours, the silence efficiency of siRNAs was detected using qPCR analysis.

### **Western blotting assays**

The lysates of the indicated cells were prepared from 6-well plates, separated on 10% SDS-PAGE gels and transferred to polyvinylidene fluoride membranes (PVDF, Thermo Fisher Scientific), which were incubated with the specific antibodies against DUSP4, Beclin1, LC3B and β-actin (Cell Signaling Technology, MA, USA). Horseradish peroxidase (HRP)-linked secondary antibodies were applied to visualize the immunoreactivity under a chemiluminescence system (Omega Lum G, Aplegen, CA, USA).

## Quantitative real-time PCR (qPCR) assays

The total RNA was extracted and purified by the TRIzol method. Synthesis of cDNA and qRT-PCR measurements were performed according to the manufacturer's protocols. The pre-designed primer sequences for qPCR were as follows:

DUSP4, 5'-CTACATCCTAGGTTCCGGTCAAC-3' (sense) and

5'-TAGACGATGACCGCCGAGTA-3' (anti-sense);

GAPDH, 5'-CCTGCCTCTACTGGCGCTGC-3' (sense) and 5'-GCAGTGGGGACACGGAAGGC-3' (anti-sense).

Relative expression was calculated using the  $2^{-\Delta\Delta C_t}$  method.

GAPDH was used as the internal reference. qPCR was carried out using SYBR Premix Ex Taq™ kit (TakaRa, Tokyo, Japan) and ABI7500 PCR system (Applied Biosystems, Thermo, MA, USA).

## Cell proliferation analysis

To assess the cell proliferation, cell counting Kit-8 (CCK-8) assays were carried out using the CCK-8 kit (Dojindo, Kumamoto, Japan). For CCK-8 assay, the indicated cells were plated into 96-well plates with 2,500 cells/well. Following the indicated time, all cells were incubated with 10  $\mu$ l CCK-8 reagent. After 2 h incubation, the optical density at 450 nm (OD450) was measured using Varioskan Flash reader (Thermo Fisher Scientific).

## Cell death analysis

To evaluate the cell death, trypan blue exclusion assays were performed as previously described<sup>19</sup>. The cells failing to exclude the presented blue-dye were defined as the dead cells. The total death rate (%) = number of dead cells/(number of living cells + number of dead cells)  $\times$  100%.

## Immunofluorescence assays

The indicated cells were seeded on 6-cm dishes and fixed using 4% paraformaldehyde (PFA). After perforated with 0.5% Triton-100, cells were blocked using 1% bovine serum albumin (BSA) and incubated with the specific antibody against LC3B (Cell Signaling Technology) at 4°C overnight. Subsequently, cells were stained with fluorochrome-labelled secondary antibody for 30 min and then counterstained with DAPI for 10 min. Ultimately, the cells were observed and counted under the fluorescence microscopy (Olympus IX81, Tokyo, Japan). The cells with more than five LC3-puncta were considered positive cells [31].

## Cell migration assays

The migratory ability of cells was evaluated by Transwell assay. For Transwell assay, the indicated cells suspended in serum-free DMEM along with 1mg/ml mitomycin C (aimed to inhibit cell proliferation) were

seeded onto the upper chamber of the Transwell. DMEM containing 20% FBS was added into the lower chamber. After 36 h of incubation, the cells that migrated to the lower surface of the inserts were fixed, stained with 1% crystal violet, and photographed. The migration levels were determined by counting the number of stained cells.

## **Animal experiments**

6-week-old male athymic BALB/c nude mice (20–22.5 g) were purchased from Animal center of Gem Pharmatech Co., Ltd (Nanjing, China). LV-DUSP4-transduced and corresponding control K1 cells were inoculated subcutaneously on the ventral side of the right rib at the density of  $5 \times 10^6$  cells per mouse (8 mice per group). According to the application of TAT-Beclin1 peptide and the transduced lentiviruses, the above tumor-bearing mice were divided into four groups: 1) LV-Cont group; 2) LV-Cont+TAT-Beclin1 group; 3) LV-DUSP4 group; 4) LV-DUSP4+TAT-Beclin1 group. The tumor volumes in the four groups of mice were measured every three days to observe the growth of tumours. The shortest diameter (A) and the longest diameter (B) were measured with a caliper to determine the tumour volume. The volume was calculated using the formula  $V = (A^2 \times B)/2$ . After 30 days, all mice were anesthetized with isoflurane (2%, Inhalation anesthesia), and then sacrificed via cervical dislocation. All mice were considered dead when their hearts and breathings stopped. Their tumours were removed and weighted. These experimental protocols were approved by the Institutional Animal Care and Use Committee of The Second Affiliated Hospital of Hebei Medical University (2016-R269). The mice were housed in a specific pathogen-free facility with barrier in which the room temperature was 20~30°C and the humidity 60~80% and fed a SPF mouse chow and sterile water.

## **Immunohistochemistry (IHC) assessment**

The tissue sections were prepared, incubated overnight at 4°C with primary DUSP4 antibody (1:100), and then visualized by the PV-9000 DAB detection kit in accordance with manufacturer's protocols. The sections were observed under the IX81 microscope. DUSP4 staining was graded semi-quantitatively. Staining intensity was graded as 1 (no stain), 2 (weak stain), 3 (clear stain), or 4 (strong stain). The total immunoreactivity score was obtained by multiplying the intensity and abundance (expressed as a fraction).

## **Statistical analysis**

All statistical analyses were performed using the GraphPad Prism Software 6. For comparisons, Wilcoxon rank sum test, one-way ANOVA test or Student's *t*-test were performed as indicated. Tukey test was used for Post-Hoc Multiple Comparisons. Pearson chi-square test were performed for correlations.  $P < 0.05$  was considered statistically significant.

# **Results**

# The expression of LC3II and Beclin1 decreased in PTC carcinoma tissues with high DUSP4 expression

Firstly, the GEPIA of TCGA database showed that the expression levels of DUSP4 in esophageal cancer tissues was significantly higher than that in adjacent tissues (Fig. 1A). According to DUSP4 expression levels, 45 ESCC cancer tissues were divided into three groups by the immunohistochemical results (Fig. 1B). It was shown that DUSP4 levels in the three groups increased in turn (Fig. 1C). The correlation analyses regarding clinical data showed that high DUSP4 levels was positively correlated with the growth, aggressiveness and metastasis of PTC cancer tissues (**Table 1**). As shown in Fig. 1D, E, the protein expression of Beclin1 and LC3II decreased in turn. It was indicated that the increase of DUSP4 was accompanied by the decrease of autophagy proteins, Beclin1 and LC3II, in ESCC tissues.

## The autophagy inhibited by DUSP4 overexpression was reversed by treatment of TAT-Beclin1 in PTC cells

Next, we verified the effect of TAT-Beclin1 on the autophagy of PTC cells regulated by DUSP4 *in vitro*. As shown in Fig. 2A, B, DUSP4 overexpression decreased the LC3 transformation rate (The ratio of LC3II/LC3I) in PTC cell lines (K1, TPC-1), which was reversed by TAT-Beclin1 administration. Similarly, DUSP4 overexpression attenuated the LC3-puncta formation in K1 and LC3, which was also reversed by TAT-Beclin1 administration (Fig. 2C-F). These results suggested that TAT-Beclin1 could compensate the autophagy of PTC cells inhibited by DUSP4.

## The proliferation and migration promoted by DUSP4 overexpression were reversed by treatment of TAT-Beclin1 in PTC cells

We documented that TAT-Beclin1 could recover the autophagic activity of PTC cells inhibited by DUSP4. The effect of TAT-Beclin1 on the survival, proliferation and function of PTC cells regulated by DUSP4 should be further clarified. As shown in Fig. 3A, C, the total death of K1 and TPC-1 cells inhibited by DUSP4 overexpression was reversed by TAT-Beclin1 administration. In addition, the proliferation levels of K1 and TPC-1 cells promoted by DUSP4 overexpression was also reversed by TAT-Beclin1 administration (Fig. 3B, D). Moreover, the migratory ability of K1 and TPC-1 cells promoted by DUSP4 overexpression was also reversed by TAT-Beclin1 administration (Fig. 3E-H). It was suggested that TAT-Beclin1 could recover the proliferation and migration of PTC cells promoted by DUSP4. Remarkably, DUSP4 knockdown-promoted the total death and -inhibited the proliferation of K1 and TPC-1 cells were not affected by TAT-Beclin1 administration (**Supplementary FigS.S1**).

## The tumorigenesis of PTC cells promoted by DUSP4 overexpression was reversed by treatment of TAT-Beclin1

The effect of TAT-Beclin1 on tumorigenicity of PTC cells regulated by DUSP4 *in vivo* should be further elucidated. The import efficiency of DUSP4-overexpressed K1 cells in xenograft tumors *in vivo* was verified by the results in Fig. 4A. As shown in Fig. 4B, compared with the tumors in LV-Cont group, the tumors formed by DUSP4-overexpressed K1 cells had larger sizes. However, TAT-Beclin1 administration

reversed the increased sizes of xenograft tumors by DUSP4-overexpressed K1 cells (Fig. 4B). In addition, the tumor growth curve formed by DUSP4-overexpressed K1 cells was significantly higher than that in LV-Cont group, which was also reversed by TAT-Beclin1 administration (Fig. 4C). The alteration trend regarding the weights of removed tumors in each group was similar to the results in Fig. 4B, C (Fig. 4D). These results indicate that TAT-Beclin1 could recover the tumorigenicity of PTC cells *in vivo* promoted by DUSP4. Importantly, the protein expression of Beclin1 and LC3II in the tumors formed by DUSP4-overexpressed K1 cells significantly decreased compared with those in LV-Cont group, which was also reversed by TAT-Beclin1 administration (Fig. 4E, F). It suggested that TAT-Beclin1 could compensate for the inhibited autophagy in the tumors formed by DUSP4-overexpressed PTC cells.

## Discussion

DUSP4 can serve as a potential biomarker for PTC [7]. As a negative regulator of MAPK, DUSP4 can inhibit JNK signaling [2, 16]. JNK is widely considered to be a pro-autophagic molecule, which results into autophagic cell death of tumors [21–23]. JNK-Beclin1-autophagy signaling is a classic pathway of JNK-regulated autophagy activation [17, 24, 25]. which is also described in PTC-related research [26]. As expected, DUSP4 could inhibit Beclin1 expression and autophagic activity through inactivating MAPKs including JNK [13], which leaves an intriguing scientific question for PTC research, whether the therapeutic effect of Beclin1 recombinant protein, TAT-Beclin1, on PTC is related to DUSP4 expression in tumors. In our study, DUSP4 expression was negatively correlated with the expression of Beclin1 and LC3II in PTC cancer tissues, which implied the inhibitory effect of DUSP4 on Beclin1 levels and autophagic activity *in vivo*. Accordingly, the decrease of Beclin1 may bridge the high DUSP4 expression and autophagy inhibition. Importantly, High DUSP4 levels indicated more obvious growth, aggressiveness and metastasis in PTC cancer tissues, which suggested that inhibition of Beclin1-dependent autophagy contributes to the poor prognosis of PTC patients. The above results paved the way for further biological detection *in vivo* and *in vitro*.

As expected, DUSP4 overexpression reduced the autophagic responses and total death levels of PTC cells, which indicated that DUSP4 inhibits the autophagic death of PTC cells. The above inference was also verified by the enhancement of proliferative and migratory ability of PTC cells by DUSP4 overexpression. However, treatment of TAT-Beclin1 not only restored the autophagic activity and total death inhibited by DUSP4 overexpression, but also suppressed the proliferation and migration promoted by DUSP4 overexpression in PTC cells. These results indicated that DUSP4 signal attenuates autophagic cell death by the inhibition of Beclin1 expression, which enhances the survival and function of PTC cells. Therefore, the application of TAT-Beclin1 can significantly promote the autophagic death, whereby inhibiting the survival and function in DUSP4-overexpressed PTC cells. It was observed that the application of TAT-Beclin1 could not affect the total death levels and proliferation in DUSP4-silenced PTC cells, indicating that due to the upregulation of autophagy, DUSP4 knockdown does not leave any space for TAT-Beclin1 administration, which verified the above theory in reverse. *In vivo* assays also showed that PTC cells with overexpressed DUSP4 could form larger tumors, which was accompanied by lower expression of Beclin1 and LC3II in tumors. Nevertheless, The above *in vivo* effects of DUSP4

overexpression could be recovered by the application of TAT-Beclin1, which further confirmed the repressive effect of TAT-Beclin1 on PTC with high DUSP4 levels. **The current working model regarding the study is described in Fig. 4G.**

## Conclusion

Our study confirmed that TAT-Beclin1 can effectively repress the carcinogenesis of DUSP4-positive PTC *in vivo* and *in vitro*, which is attributed to its ability to recover the autophagic cell death of PTC inhibited by DUSP4. Based on these data, the prevention and treatment of PTC may be further improved in the future, i.e., the addition of TAT-Beclin1 can be selected according to the expression of DUSP4 in the treatment of PTC.

## Abbreviations

PTC, papillary thyroid carcinoma; DUSP4, Dual specificity phosphatase 4; MAPK, mitogen-activated protein kinase; JNK, c-Jun N-terminal kinase; ERK, extracellular regulated protein kinase; FBS, fetal bovine serum; MOI, multiplicity of infection; CCK-8, cell counting Kit-8; IHC, Immunohistochemistry; qPCR, Quantitative real-time PCR.

## Declarations

### Acknowledgements

Not applicable.

### Funding

This work was supported by The Natural Science Foundation of Hebei Province (H2018206180).

### Authors' contributions

N.H. and L.Z. conceived and designed experiments; L.Z. and Y.S. performed experiments, analyzed data, and prepared figures; Y.T. helped with analysis of the data; L.Z. and N.H. wrote the manuscript.

### Availability of data and materials

All our data generated or analysed during this study are included in this published article. And all data used to support the findings of this study are available from the corresponding author upon reasonable request.

### Ethics approval and consent to participate

The present study protocol was approved by the Research Ethics Committee of The second hospital of Hebei Medical University (Shujiazhuang, Hebei, China) and written informed consent was obtained from

all the participants for their tissues to be used for the purposes of this research.

### **Patient consent for publication**

Not applicable.

### **Competing interests**

All authors declared that they have no competing interests.

### **Author details**

<sup>1</sup>Department 5 of General Surgery, The second hospital of Hebei Medical University, Shijiazhuang, 050005, Hebei, China. <sup>2</sup>Department of infection management/public health, Hebei People's Hospital, Shijiazhuang, 050057, Hebei, China. <sup>3</sup>Department 2 of Oncology, The second hospital of Hebei Medical University, Shijiazhuang, 050005, Hebei, China. <sup>4</sup>Department 4 of General Surgery, The second hospital of Hebei Medical University, Shijiazhuang, 050005, Hebei, China

## **References**

1. Ertek S, Yilmaz NC, Cicero AF, Vurupalmaz Ö, Demiröz AS, Erdoğan G. Increasing diagnosis of thyroid papillary carcinoma follicular variant in south-east Anatolian region: comparison of characteristics of classical papillary and follicular variant thyroid cancers. *Endocr Pathol.* 2012;23(3):157–60.
2. Balko JM, Schwarz LJ, Bholra NE, Kurupi R, Owens P, Miller TW, Gómez H, Cook RS, Arteaga CL. Activation of MAPK pathways due to DUSP4 loss promotes cancer stem cell-like phenotypes in basal-like breast cancer. *Cancer Res.* 2013;73(20): 6346–58.
3. Hijjiya N, Tsukamoto Y, Nakada C, Tung Nguyen L, Kai T, Matsuura K, Shibata K, Inomata M, Uchida T, Tokunaga A, *et al.* Genomic Loss of DUSP4 Contributes to the Progression of Intraepithelial Neoplasm of Pancreas to Invasive Carcinoma. *Cancer Res.* 2016;76(9): 2612–25.
4. Schmid CA, Robinson MD, Scheifinger NA, Müller S, Cogliatti S, Tzankov A, Müller A. DUSP4 deficiency caused by promoter hypermethylation drives JNK signaling and tumor cell survival in diffuse large B cell lymphoma. *J Exp Med.* 2015;212(5):775–92.
5. Xu X, Gao F, Wang J, Tao L, Ye J, Ding L, Ji W, Chen X. MiR-122-5p inhibits cell migration and invasion in gastric cancer by down-regulating DUSP4. *Cancer Biol Ther.* 2018;19(5):427–35.
6. Gröschl B, Bettstetter M, Giedl C, Woenckhaus M, Edmonston T, Hofstädter F, Dietmaier W. Expression of the MAP kinase phosphatase DUSP4 is associated with microsatellite instability in colorectal cancer (CRC) and causes increased cell proliferation. *Int J Cancer.* 2013;132(7):1537–46.
7. Ma B, Shi R, Yang S, Zhou L, Qu N, Liao T, Wang Y, Wang Y, Ji Q. DUSP4/MKP2 overexpression is associated with BRAF(V600E) mutation and aggressive behavior of papillary thyroid cancer. *Oncotargets Ther.* 2016;9:2255–63.

8. Abraham MC, Shaham S. Death without caspases, caspases without death. *Trends Cell Biol.* 2004;14(4):184–93.
9. Liang XH, Jackson S, Seaman M, Brown K, Kempkes B, Hibshoosh H, Levine B. Induction of autophagy and inhibition of tumorigenesis by beclin 1. *Nature.* 1999;402(6762):672–6.
10. Kim TW, Lee SY, Kim M, Cheon C, Ko SG. Kaempferol induces autophagic cell death via IRE1-JNK-CHOP pathway and inhibition of G9a in gastric cancer cells. *Cell Death Dis.* 2018;9(9):875.
11. Zhang G, He J, Ye X, Zhu J, Hu X, Shen M, Ma Y, Mao Z, Song H, Chen F.  $\beta$ -Thujaplicin induces autophagic cell death, apoptosis, and cell cycle arrest through ROS-mediated Akt and p38/ERK MAPK signaling in human hepatocellular carcinoma. *Cell Death Dis.* 2019;10(4):255.
12. Choi JC, Wu W, Muchir A, Iwata S, Homma S, Worman HJ. Dual specificity phosphatase 4 mediates cardiomyopathy caused by lamin A/C (LMNA) gene mutation. *J Biol Chem.* 2012;287(48):40513–24.
13. Han W, Fu X, Xie J, Meng Z, Gu Y, Wang X, Li L, Pan H, Huang W. MiR-26a enhances autophagy to protect against ethanol-induced acute liver injury. *J Mol Med (Berl).* 2015;93(9):1045–55.
14. Barajas-Espinosa A, Basye A, Angelos MG, Chen CA. Modulation of p38 kinase by DUSP4 is important in regulating cardiovascular function under oxidative stress. *Free Radic Biol Med.* 2015;89:170–81.
15. Kim SY, Han YM, Oh M, Kim WK, Oh KJ, Lee SC, Bae KH, Han BS. DUSP4 regulates neuronal differentiation and calcium homeostasis by modulating ERK1/2 phosphorylation. *Stem Cells Dev.* 2015;24(6):686–700.
16. Denhez B, Rousseau M, Dancosst DA, Lizotte F, Guay A, Auger-Messier M, Côté AM, Gervais P. Diabetes-Induced DUSP4 Reduction Promotes Podocyte Dysfunction and Progression of Diabetic Nephropathy. *Diabetes.* 2019;68(5):1026–39.
17. Wei Y, Pattingre S, Sinha S, Bassik M, Levine B. JNK1-mediated phosphorylation of Bcl-2 regulates starvation-induced autophagy. *Mol Cell.* 2008;30(6):678–88.
18. Pattingre S, Bauvy C, Levade T, Levine B, Codogno P. Ceramide-induced autophagy: to junk or to protect cells? *Autophagy.* 2009;5:558–60.
19. Ni Z, Wang B, Dai X, Ding W, Yang T, Li X, Lewin S, Xu L, Lian J, He F. HCC cells with high levels of Bcl-2 are resistant to ABT-737 via activation of the ROS-JNK-autophagy pathway. *Free Radic Biol Med.* 2014;70:194–203.
20. Liu YW, Yang T, Zhao L, Ni Z, Yang N, He F, Dai SS. Activation of Adenosine 2A receptor inhibits neutrophil apoptosis in an autophagy-dependent manner in mice with systemic inflammatory response syndrome. *Sci Rep.* 2016;6:33614.
21. Nazim UM, Yin H, Park SY. Neferine treatment enhances the TRAIL-induced apoptosis of human prostate cancer cells via autophagic flux and the JNK pathway. *Int J Oncol.* 2020;56(5):1152–61.
22. Liu S, Lin H, Wang D, Li Q, Luo H, Li G, *et al.* PCDH17 increases the sensitivity of colorectal cancer to 5-fluorouracil treatment by inducing apoptosis and autophagic cell death. *Signal Transduct Target Ther.* 2019;4(1):53.

23. Zhou N, Wei Z, Qi Z, Chen L. Abscisic Acid-Induced Autophagy Selectively via MAPK/JNK Signalling Pathway in Glioblastoma. *Cell Mol Neurobiol*. 2020. doi: 10.1007/s10571-020-00888-1.
24. Qin X, Lu A, Ke M, Zhu W, Ye X, Wang G, Weng G. DJ-1 inhibits autophagy activity of prostate cancer cells by repressing JNK-Bcl2-Beclin1 signaling. *Cell Biol Int*. 2020;44(4):937–46.
25. Park KJ, Lee SH, Lee CH, Jang JY, Chung J, Kwon MH, Kim YS. Upregulation of Beclin-1 expression and phosphorylation of Bcl-2 and p53 are involved in the JNK-mediated autophagic cell death. *Biochem Biophys Res Commun*. 2009;382(4):726–9.
26. He H, Du Z, Lin J, Wu W, Yu Y. DUSP4 inhibits autophagic cell death in PTC by inhibiting JNK-BCL2-Beclin1 signaling. *Biochem Cell Biol*. 2021; Doi: 10.1139/bcb-2020-0636.
27. Shoji-Kawata S, Sumpter R, Leveno M, Campbell GR, Zou Z, Kinch L, *et al*. Identification of a candidate therapeutic autophagy-inducing peptide. *Nature*. 2013;494(7436):201–6.
28. Sun Y, Yao X, Zhang QJ, Zhu M, Liu ZP, Ci B, Xie Y, Carlson D, Rothermel BA, Sun Y, Levine B, Hill JA, Wolf SE, Minei JP, Zang QS. Beclin-1-Dependent Autophagy Protects the Heart During Sepsis. *Circulation*. 2018;138(20):2247–62.
29. Atwood DJ, Pokhrel D, Brown CN, Holditch SJ, Bachu DM, Thorburn A, Hopp K, Edelstein CL. Increased mTOR and suppressed autophagic flux in the heart of a hypomorphic Pkd1 mouse model of autosomal dominant polycystic kidney disease. *Cell Signal*. 2020;74:109730.
30. Karakashev S, Zhu H, Wu S, Yokoyama Y, Bitler BG, Park PH, Lee JH, Kossenkov AV, Gaonkar KS, Yan H, Drapkin R, Conejo-Garcia JR, Speicher DW, Ordog T, Zhang R. CARM1-expressing ovarian cancer depends on the histone methyltransferase EZH2 activity. *Nat Commun*. 2018;9(1):631.
31. Wang X, Qi H, Wang Q, Zhu Y, Wang X, Jin M, Tan Q, Huang Q, Xu W, Li X, Kuang L, Tang Y, Du X, Chen D, Chen L. FGFR3/fibroblast growth factor receptor 3 inhibits autophagy through decreasing the ATG12–ATG5 conjugate, leading to the delay of cartilage development in achondroplasia. *Autophagy*. 2015;11(11):1998–2013.

## Tables

### Table 1

Correlation between DUSP4 levels and clinicopathological characteristics of papillary thyroid carcinoma (PTC) patients.

Characteristics	Case	DUSP4			P value
		L	M	H	
<b>Total</b>	45	15	15	15	
<b>Gender</b>					0.7111
Male	12	3	5	4	
Female	33	12	10	11	
<b>Age</b>					0.6977
≥ 65	20	6	8	6	
< 65	25	9	7	9	
<b>CDFI classification grade</b>					0.0303*
I	28	13	9	6	
II-III	17	2	6	9	
<b>Degree of invasion</b>					0.0128*
Intrathyroid	22	11	8	3	
Extrathyroid	23	4	7	12	
<b>PTC diameter</b>					0.0117*
≥ 3.0cm	27	5	9	13	
< 3.0cm	18	10	6	2	
<b>Pathological stage (T)</b>					0.0138*
T2	24	12	8	4	
T3-pT4	21	3	7	11	
<b>Pathological stage (N)</b>					0.0004*
N0	32	14	13	5	
N1	13	1	2	10	
<b>Outcome</b>					0.1693
Persisted/recurrent	2	2	0	0	
Death	1	1	0	0	
Cured	42	12	15	15	

P value was acquired by Pearson chi-square test.

## Figures

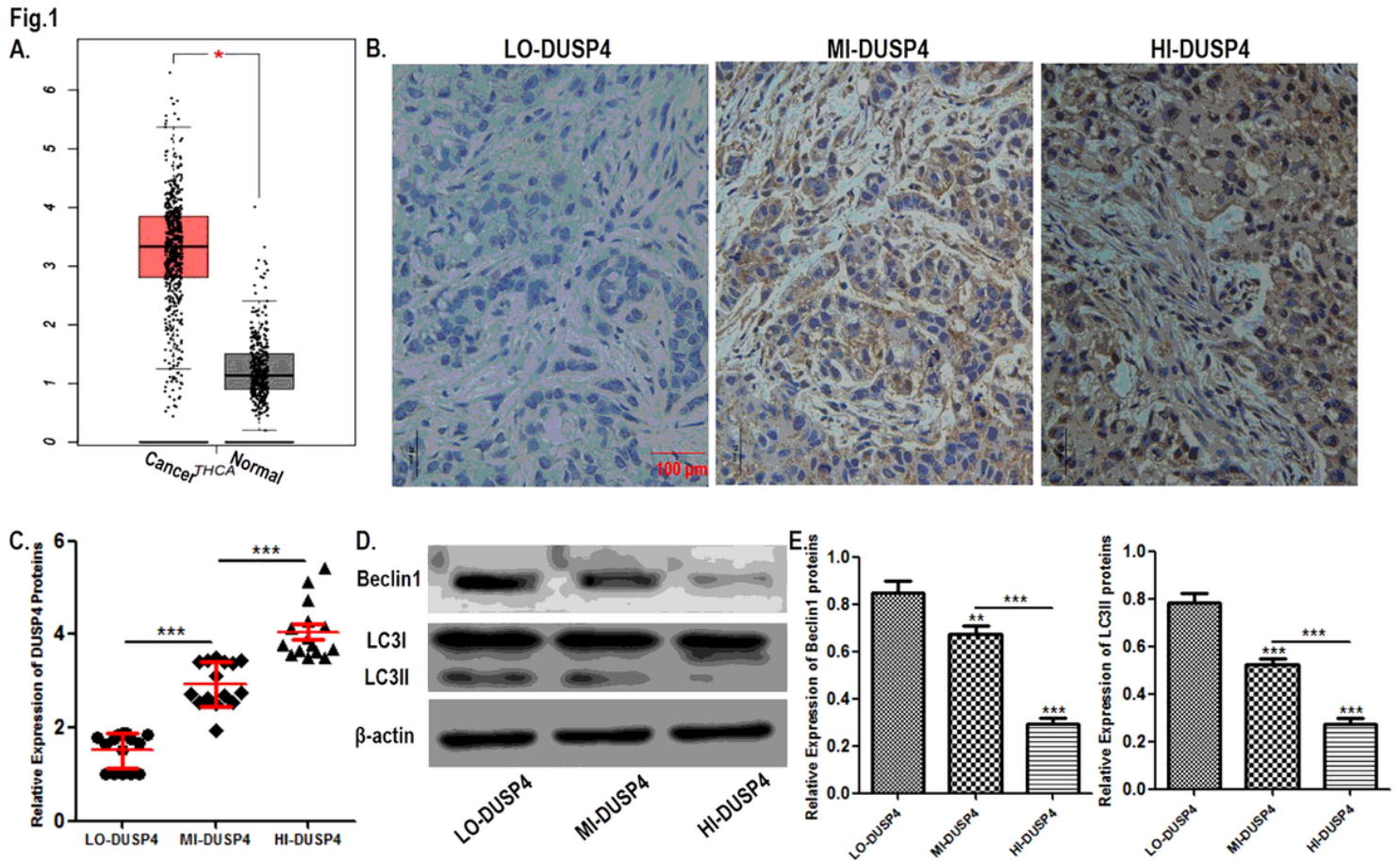


**Figure 1**

The expression of LC3II and Beclin1 decreased in PTC carcinoma tissues with high DUSP4 expression. (A) mRNA abundance analysis of DUSP4 gene in GEPIA database (<http://gepia.cancer-pku.cn/index.html>). (B) Immunohistochemical analysis of PTC cancer tissues with low DUSP4 levels, moderate DUSP4 levels, high DUSP4 levels (15 per group). Scale bar, 100 μm. (C) The quantitative results of immunohistochemical staining in B (n=15). (D-E) The protein expressions of Beclin1 and LC3II of each group in B were detected by Western blotting (n=15). Results are presented as mean±SEM. \*\*P<0.01, \*\*\*P<0.001 by one-way ANOVA test. LO-DUSP4, low DUSP4 levels; MI-DUSP4, moderate DUSP4 levels; HI-DUSP4, high DUSP4 levels.

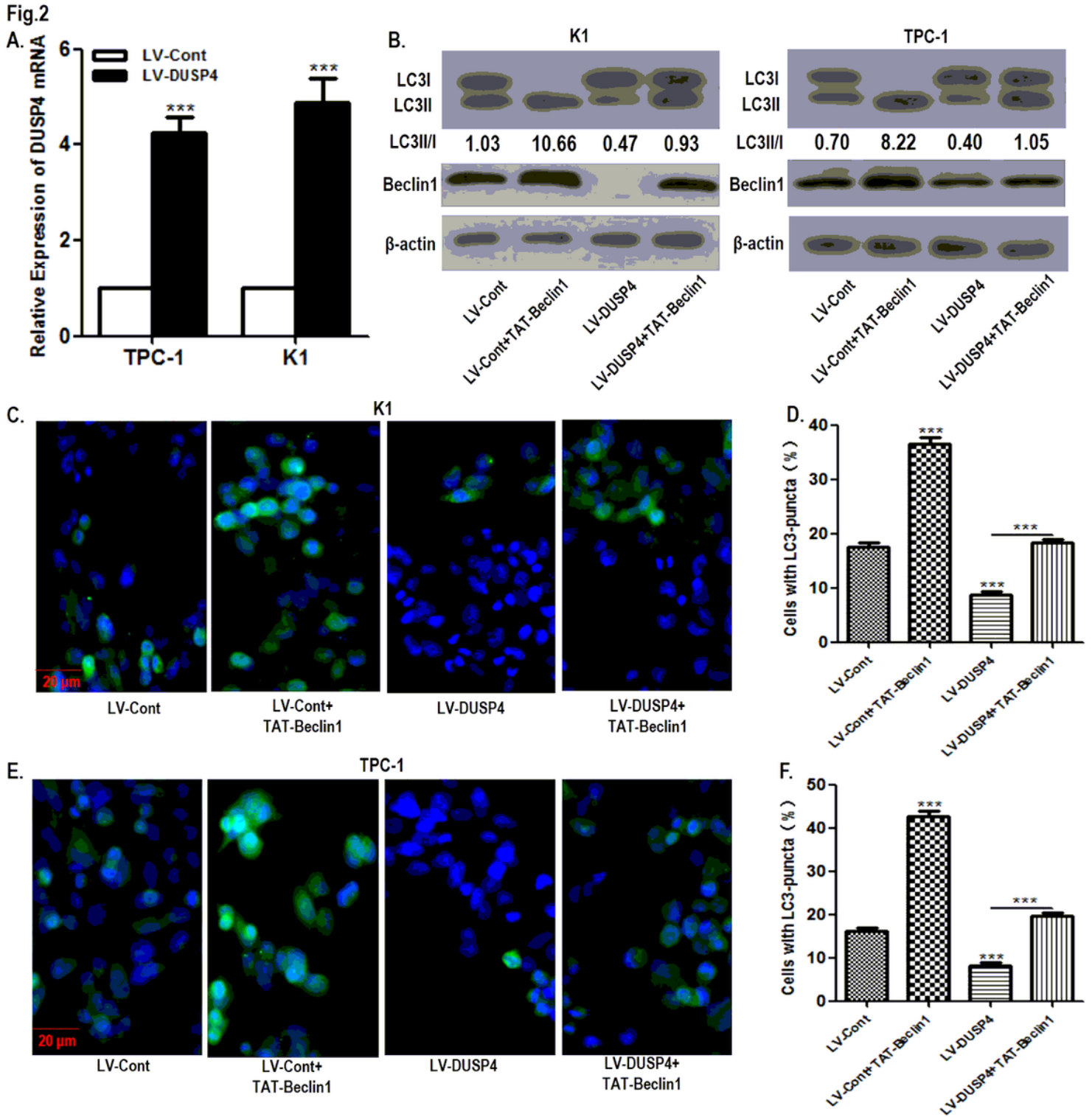


**Figure 2**

The autophagy inhibited by DUSP4 overexpression was reversed by treatment of TAT-Beclin1 in PTC cells. (A) DUSP4 mRNA levels in TPC-1 and K1 cells transduced with lentiviruses encoding DUSP4 (LV-DUSP4) or corresponding control vector (LV-Cont). (B) LC3 transformation (the ratio of LC3II/I) and Beclin1 protein expression in lentiviruses-transduced K1 and TPC-1 cells treated with TAT-Beclin1 for 8 h were detected by Western blotting. (C, E) LC3 puncta (yellow fluorescence) in treated K1 and TPC-1 cells was imaged using

immunofluorescence staining and observed under fluorescence microscopy. Scale bar, 20  $\mu\text{m}$ . (D, F) The histogram showing the percentages of cells with LC3 puncta in C, E ( $\geq 5$  dots, 50 cells per field,  $n=5$ ). Results are presented as mean $\pm$ SEM from three independent experiments. \*\*\* $P<0.001$  by one-way ANOVA test.

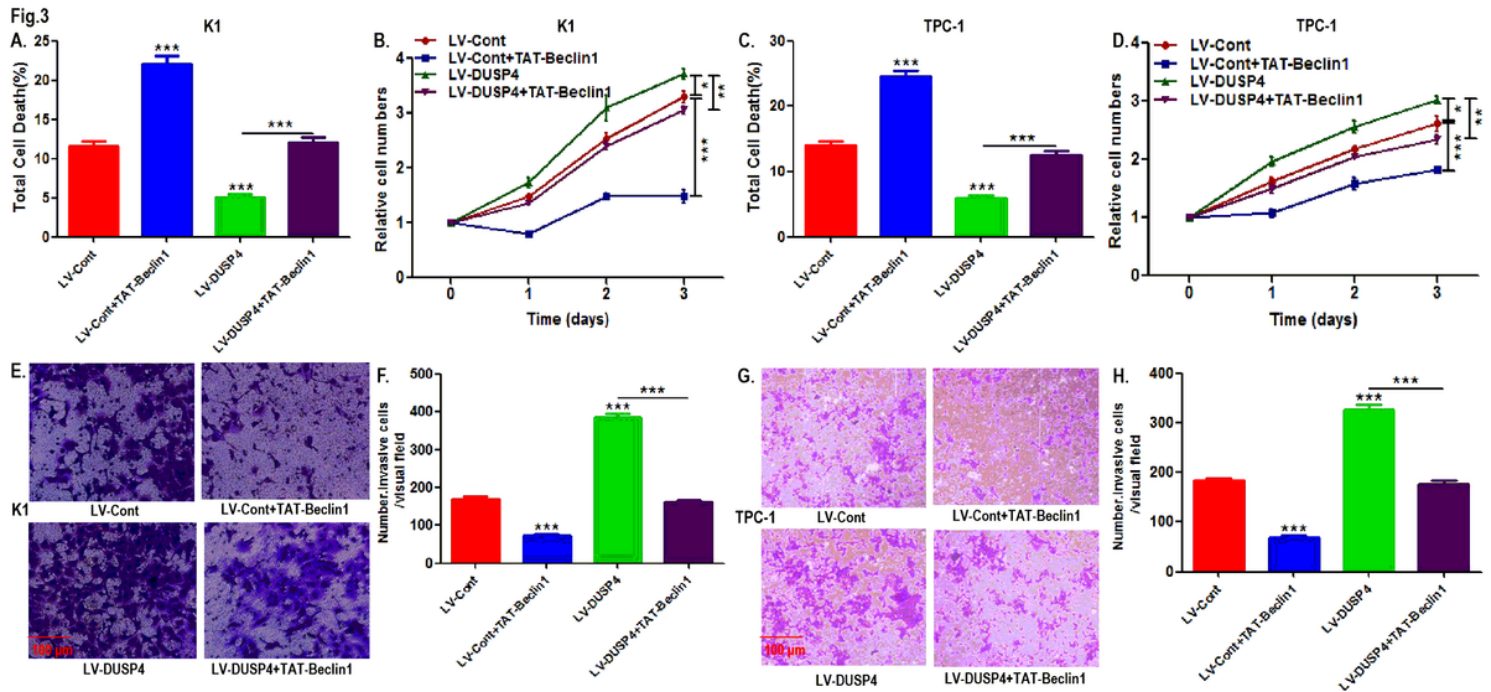


**Figure 3**

The proliferation and migration promoted by DUSP4 overexpression were reversed by treatment of TAT-Beclin1 in PTC cells. (A, C) The total death levels of lentiviruses-transduced K1 and TPC-1 cells treated with TAT-Beclin1 for 24 h were evaluated by trypan blue staining. (B, D) The proliferation of treated K1 and TPC-1 cells was evaluated by CCK-8 assays. (E-H) The migration of treated K1 and TPC-1 cells was assessed by Transwell assays. Scale bar, 100  $\mu\text{m}$ . Results are presented as mean $\pm$ SEM from three independent experiments. \* $P<0.05$ , \*\* $P<0.01$ , \*\*\* $P<0.001$  by one-way ANOVA test.

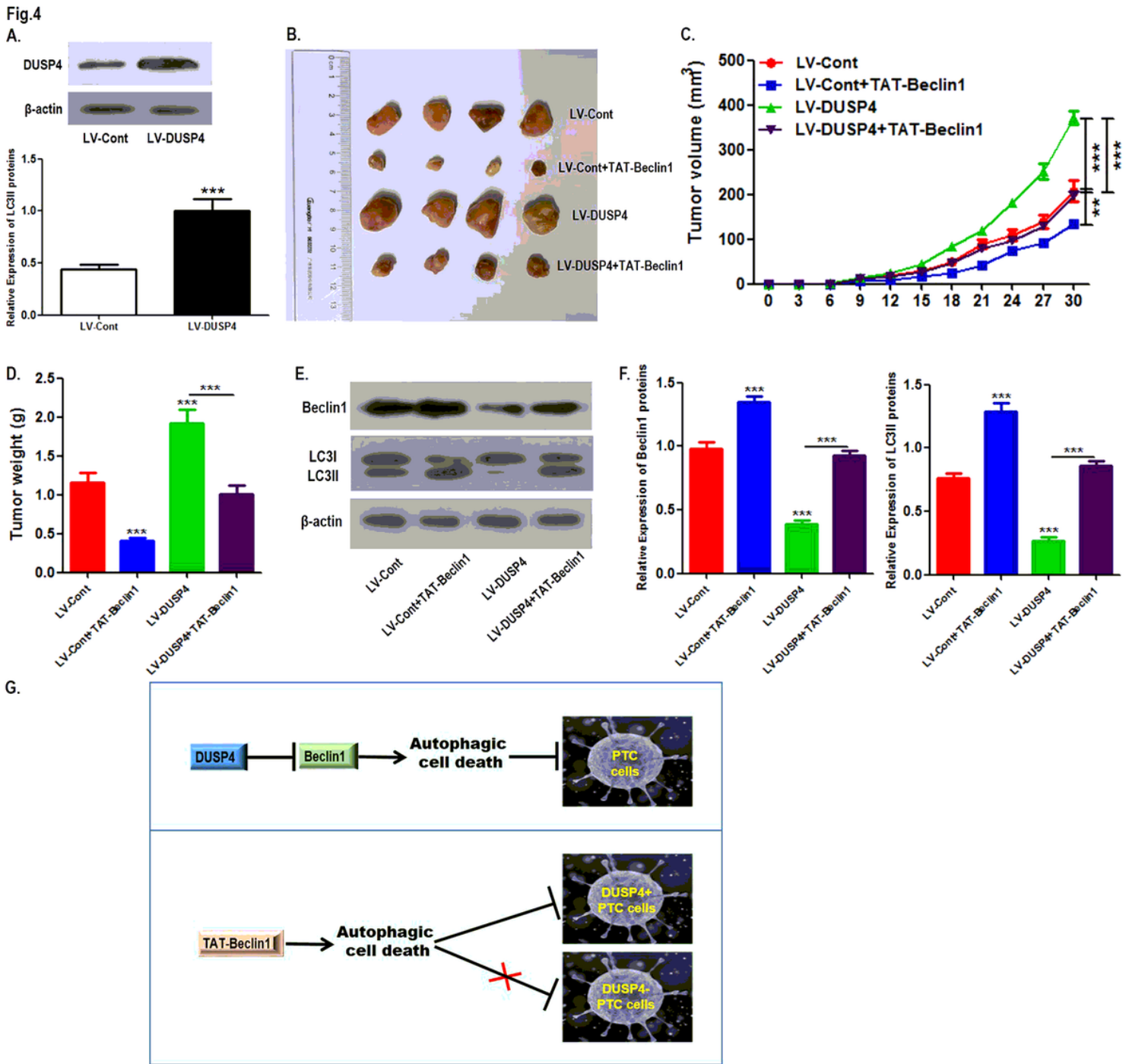


**Figure 4**

The tumorigenesis of PTC cells promoted by DUSP4 overexpression was reversed by treatment of TAT-Beclin1. DUSP4-overexpressed or corresponding control K1 cells was inoculated into nude mice, and then lentiviruses-transduced cells were treated with TAT-Beclin1. 30 days later, all tumor-bearing mice were killed, and tumors were removed and weighted. (A) Protein levels of DUSP4 in xenograft tumor tissues were assessed using Western blotting (N=8). (B) Representative images of the removed tumors at week 4. (C) The scatter plot indicates tumor growth curves of four groups from day 0-30 (N=8). (D) The histogram indicates the quantitative results regarding the weight of removed tumors (N=8). (E,F) Protein levels of Beclin1 and LC3II in xenograft tumor tissues were assessed using Western blotting (N=8). (G) The

working model regarding the role of TAT-Beclin1-mediated autophagic death in DUSP4-regulated PTC carcinogenesis. Results are presented as mean±SEM. \*\*P<0.01, \*\*\*P<0.001 by one-way ANOVA test.

## Supplementary Files

This is a list of supplementary files associated with this preprint. Click to download.

- [Supplementarymaterials.doc](#)